Synthesis of Activated Carbons from Corncob Biomass Waste as Electrode Materials for Supercapacitors

Chanatip Sungprasit[1,2], Kasidit Janbooranapinij[1,2], Nonthapat Kosacarn[1], Attanon Choomthi[1], Gasidit Panomsuwan[1,2,*]

[1] Department of Materials Engineering, Faculty of Engineering, Kasetsart University, Bangkok 10900, Thailand
[2] Special Research Units for Biomass Conversion Technology for Energy and Environmental Materials, Kasetsart University, Bangkok 10900, Thailand
*gasidit.p@ku.ac.th

Abstract. Nowadays, activated carbons (ACs) derived from biomass waste are promising materials for various applications, particularly supercapacitors, due to their high surface area and porosity, low cost, natural abundance, power delivery performance, and electrochemical stability. In this work, ACs were synthesized from corncob waste through carbonization at 600 °C followed by chemical activation using zinc chloride ($ZnCl_2$) at 800 °C in various ratios: 1:1, 1:2, 1:3, and 1:4. The characterization results revealed that ACs exhibited an amorphous carbon phase without any impurities and had almost no chemical functional groups. The morphology of the ACs showed the development of a porous structure compared to raw corncob and non-activated samples. The specific surface area of ACs slightly increased from 417 to 450 $m^2 g^{-1}$ with the increasing $ZnCl_2$ content, mainly due to the development of micropores, with a smaller proportion of meso-macropores. The electrochemical properties of ACs were characterized using a three-electrode system in a 6 M KOH electrolyte via cyclic voltammetry (CV) and galvanostatic charge-discharge (GCD). The AC synthesized using a ratio of 1:4 showed the highest specific capacitance of 56 F g^{-1} attributed to its highest specific surface area. Additionally, the capacitance retention remained at 92% after 5,000 cycles. This study provides valuable information on converting corncob waste into ACs as electrode materials in supercapacitor applications.

Keywords: Corncob, Biomass, Activated carbons, Supercapacitors.

1 Introduction

Currently, energy development encompasses various forms, such as solar and wind energy, which are driving the advancement of energy storage systems like rechargeable batteries and supercapacitors [1]. These devices allow for storing energy based on the application and specific requirements. Among the diverse energy storage devices, batteries and fuel cells are notable for their ability to store substantial amounts of energy, though they deliver it at a slow rate [2]. Supercapacitors offer distinct

advantages, such as high-power density, long cycle life (>100,000 cycles), and enhanced safety. They are utilized in diverse fields, including powering hybrid and electric vehicles, smart grids, UPS systems, and a wide range of consumer electronics [3]. The energy storage mechanisms of supercapacitors are typically categorized into three types: (i) electrochemical double-layer capacitors (EDLCs), (ii) pseudocapacitors, and (iii) hybrid supercapacitors [4]. The choice of electrode type plays a crucial role in determining capacitance and charge storage efficiency, influenced by several factors such as specific surface area, pore structure, surface chemistry, and electrical conductivity [5]. Pseudocapacitive materials often exhibit higher specific capacitance than EDLCs due to their higher energy density. However, EDLCs with carbon-based electrodes offer superior cycle stability, and rate capability, and can operate at higher charge/discharge rates with a longer lifetime [6].

Activated carbons (ACs) are widely favored as electrode materials for supercapacitors due to their unique properties, including low cost, large specific surface area, microporosity, high conductivity, and chemical stability [7]. They can be synthesized through the carbonization and activation processes. These processes yield ACs rich in micropores, which are highly suitable for supercapacitor applications [8]. In recent years, plants, abundant in cellulose, hemicellulose, protein, lignin, starch, and other carbonaceous substances, have served as a viable source for synthesizing ACs [9]. Numerous studies have demonstrated that biomass-derived ACs offer diverse sources, low production costs, and environmental friendliness. Their porous structures provide active sites crucial for effective electrode materials in supercapacitors. The structural variability inherent in biomass results in ACs with a range of morphologies, structures, porosities, and electrochemical properties [10].

In this study, ACs were synthesized by first carbonizing at 600 °C followed by activation using $ZnCl_2$ as the activating agent at 800 °C. The resulting ACs were characterized comprehensively by various instruments to investigate their morphology, porosity, structure, and chemical functionality. Furthermore, the electrochemical charge storage capabilities of ACs were evaluated using a three-electrodes system at room temperature in a 6 M KOH electrolyte.

2 Experimental

2.1 Materials

Zinc chloride ($ZnCl_2$, 98% purity) was purchased from DAEJUNG Co., Ltd. Ethanol (C_2H_2OH, 99.9% purity) and isopropanol (C_3H_8O, 99.8% purity) were purchased from RCI Labscan Ltd. Hydrochloride acid (HCl, 37%) was purchased from Qrëc Chemical, Co., Ltd. Nafion® solution (5% wt in a mixture of water and alcohols) was purchased from Fuel Cell Earth Co., Ltd. All chemicals used in this study were of analytical grade.

2.2 Synthesis of Activated Carbons (ACs)

Corncob waste was initially dried at 105 °C for 12 h and then ground using a grinding machine. The resulting dried and ground corncob powder was carbonized at 600 °C for

3 h under 0.2 L min^{-1} Ar flow, yielding non-activated carbon (non-AC). For the activation process, $ZnCl_2$ was dissolved in water and mixed with the non-AC under magnetic stirring for 1 h, followed by drying at 105 °C for 24 h. The weight ratio of the non-AC to $ZnCl_2$ varied at 1:1, 1:2, 1:3, and 1:4. Subsequently, the mixed samples were subjected to a tube furnace for activation at 800 °C for 1 h under a 0.2 L min^{-1} Ar flow. After activation, the products were washed with 1 M HCl and deionized water until the filtrate reached a pH of 7, followed by drying at 105 °C for 24 h. The AC samples were designated based on the ratio of non-AC:$ZnCl_2$ as AC1:1, AC1:2, AC1:3, and AC1:4.

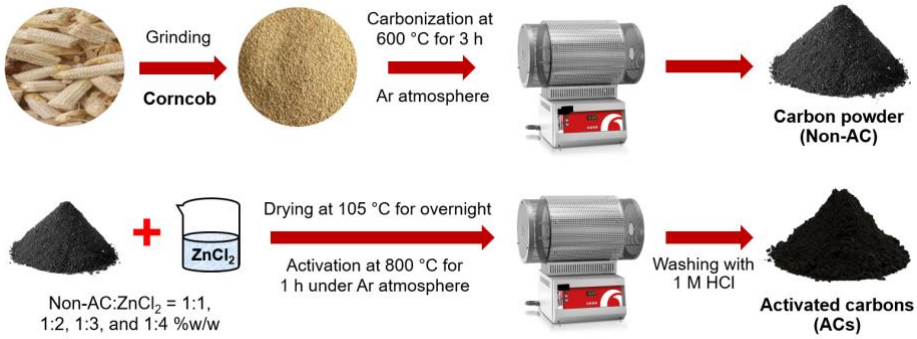

Fig. 1. Schematic illustration showing the preparation of ACs from corncob waste.

2.3 Characterization

Various analytical techniques were employed to investigate the properties of ACs. The morphology was examined using a Hitachi SU3500 scanning electron microscope. N_2 adsorption-desorption isotherms of the activated carbons were recorded at –196 °C using a Micromeritics 3Flex surface characterization analyzer to evaluate their specific surface area and pore structure. Prior to the measurement, the samples were degassed at 150 °C for 12 h under vacuum conditions. The phase structure of the ACs was verified using a PANalytical Empyrean X-ray diffractometer with Cu K_α radiation. The chemical functional group was analyzed with a Bruker Alpha-E Spectrometer in the transmittance mode, within the wavenumber range of 4000–500 cm^{-1}.

2.4 Preparation of working electrode

The ACs (5 mg) were first dispersed in a mixture comprising 475 µL ultrapure water, 475 µL isopropanol, and 50 µL Nafion. The mixture was then sonicated for 30 min to achieve a homogeneous suspension. The glassy carbon (GC) electrode was thoroughly polished on a polishing pad with diamond and alumina polishing pads. After polishing, the electrode was rinsed with deionized water and air-dried. Subsequently, 3 µL of the prepared suspension was dropped onto the GC electrode and air-dried.

2.5 Electrochemical measurements

Electrochemical measurements were performed using a three-electrodes system in a 6 M KOH electrolyte. Three electrodes included a reference electrode (Hg/HgO in 1 M NaOH), a counter electrode (Pt wire), and a working electrode. These electrodes were connected by a Biologic VSP potentiostat/galvanostat station controlled by EC-Lab software. Cyclic voltammetry (CV) measurement was performed within the potential range of 0 to –1 V at a scan rate of 100 mV s^{-1}. Galvanostatic charge-discharge (GCD) was conducted in the same potential range as the CV measurement at a current density of 1 A g^{-1}. To assess stability, charge-discharge cycling was performed for 5,000 cycles at a current density of 10 A g^{-1}.

3 Results & Discussion

3.1 Morphology

The morphology of corncob, non-AC, and ACs was investigated by scanning electron microscopy (SEM), as displayed in Fig. 2. The surface structure of both corncob and non-AC showed a ruptured surface without visible pores. However, after activation with $ZnCl_2$, a significant increase in surface porosity was observed in the AC samples compared to the corncob and non-AC samples.

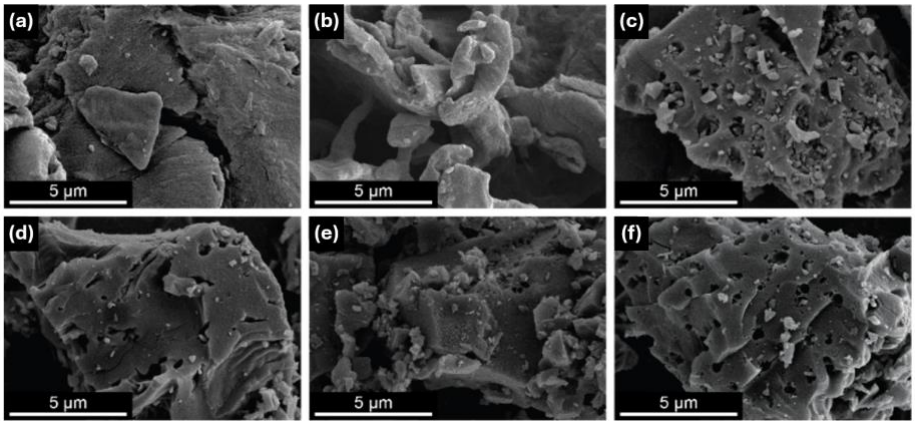

Fig. 2. SEM images: (a) corncob, (b) non-AC, (c) AC1:1, (d) AC 1:2, (e) AC1:3, and (f) AC1:4.

3.2 Surface area and porosity analysis

The N_2 adsorption-desorption isotherms of corncob and non-AC exhibited a type II feature (Fig. 3a), indicating a non-porous structure with the presence of macropores. In

contrast, the AC samples displayed a combination of type I and IV features. The initial abrupt adsorption in the isotherms corresponds to type I, indicative of micropore structures, while the hysteresis loop during desorption corresponds to type IV, suggesting mesopores with narrow slit-like shapes, as shown in Fig. 3b. The specific surface areas determined using the Brunauer–Emmett–Teller (BET) method were 416, 432, 447 and 450 $m^2 g^{-1}$ for AC1:1, AC1:2, AC1:3, and AC1:4, respectively, which was much higher than corncob (1.32 $m^2 g^{-1}$) and non-AC (1.16 $m^2 g^{-1}$). The slight increase in specific surface area was attributed to the formation of additional micropores, while the proportion of meso- and macropores remained relatively unchanged. The total pore volume and average pore diameter of ACs are listed in Table 1. These findings indicate that the increasing $ZnCl_2$ content had a slight influence on creating the porous structure and enhancing the surface area of ACs.

Table 1. The parameters obtained from N_2 adsorption-desorption analysis.

Samples	S_{BET} ($m^2 g^{-1}$)	S_{micro} ($m^2 g^{-1}$)	$S_{meso\text{-}macro}$ ($m^2 g^{-1}$)	Pore volume ($cm^3 g^{-1}$)	Pore diameter (nm)
AC1:1	417	349	68	0.032	3.51
AC1:2	432	361	71	0.035	3.54
AC1:3	447	373	74	0.040	3.69
AC1:4	450	382	68	0.035	3.82

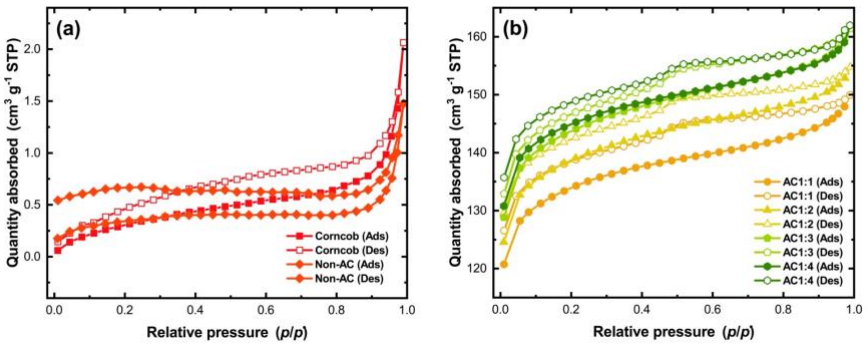

Fig. 3. N_2 adsorption-desorption isotherms of (a) corncob and non-AC and (b) AC samples (AC1:1, AC1:2, AC1:3, and AC1:4).

3.3 Phase structure

The phase structure of corncob, non-AC, and ACs was evaluated by X-ray diffraction (XRD), as shown in Fig. 4a. The XRD pattern of corncob exhibited peaks at 16.0°, 22.5°, and 34.5°, corresponding to the cellulose crystalline structure [11]. For non-AC,

the peaks associated with crystalline cellulose were absent, replaced by broad peaks of amorphous carbon at 24.3° and 43.9°, corresponding to the (002) and (101) planes, respectively. Additionally, small peaks from impurity elements of corncob were also observed. After activation with $ZnCl_2$, the XRD patterns of the ACs exhibited only amorphous carbon peaks, indicating high carbon purity and complete removal of inorganic salts from the activated products.

3.4 Chemical functional groups

The chemical functional groups were analyzed by Fourier-transform infrared spectroscopy (FTIR), as shown in Fig. 4b. The FTIR spectrum of the corncob showed absorption peaks at 3379, 2918, 1732, and 1045 cm^{-1}, corresponding to the O–H, C–H, C=O, and C–O bonds in the lignocellulosic structure, respectively [12]. After carbonization, most of these absorption peaks diminished due to the decomposition of the lignocellulosic structure and the removal of O and H at high temperatures. A peak emerging at 1566 cm^{-1} was assigned to the C=C stretching. After activation, the FTIR spectra displayed a nearly featureless profile, with only weak intensity peaks remaining. These included the O–H stretching at 3380 cm^{-1}, C=C stretching at 1525 cm^{-1}, and C–O stretching at 1098 cm^{-1}, which are the typical characteristics of ACs [13,14].

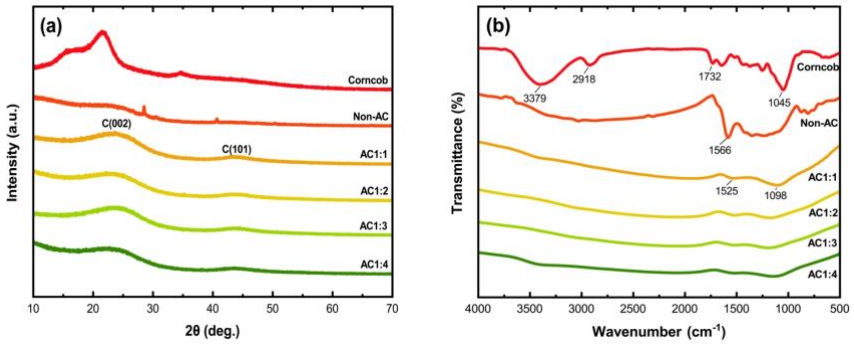

Fig. 4. (a) XRD patterns and (b) FTIR spectra of corncob, non-AC, and ACs (AC1:1, AC1:2, AC1:3, and AC1:4).

3.5 Electrochemical charge storage performance

The electrochemical properties of ACs for supercapacitor applications were evaluated in a 6 M KOH solution using CV and GCD measurements. Fig. 5a illustrates the CV curves of the ACs recorded from 0 to –1 V at a scan rate of 100 mV s^{-1}. The area of CV curves varied proportionally with the surface area of the ACs, with AC1:4 exhibiting the largest area, indicating the highest capacitance among all tested ACs. Comparative GCD curves of ACs at a current density of 1 A g^{-1} are shown in Fig. 5b, demonstrating

non-linear behavior. The specific capacitance (C_s) can be calculated using the integrated area under the discharge curve following equation [15]:

$$C_s = \frac{2I}{m(V_f - V_i)^2} \int_{V_i}^{V_f} V\, dt, \qquad (1)$$

where I is the applied current (A), m is the mass of AC, and V_f and V_i are the final and initial values of the potential range (V), respectively. At a current density of 1 A g^{-1}, C_s values were determined as 32, 37, 53, and 56 F g^{-1} for AC1:1, AC1:2, AC1:3, and AC1:4, respectively. The highest C_s value of AC1:4 can be attributed to its highest specific surface area, facilitated by increased micropore creation due to high $ZnCl_2$ content. Moreover, AC1:4 was selected for a stability test via 5,000 charge-discharge cycles at a current density of 10 A g^{-1} (Fig. 5c). The capacitance retention remained at 92% after 5,000 cycles, assessing its excellent stability and suitability for long-term supercapacitor applications.

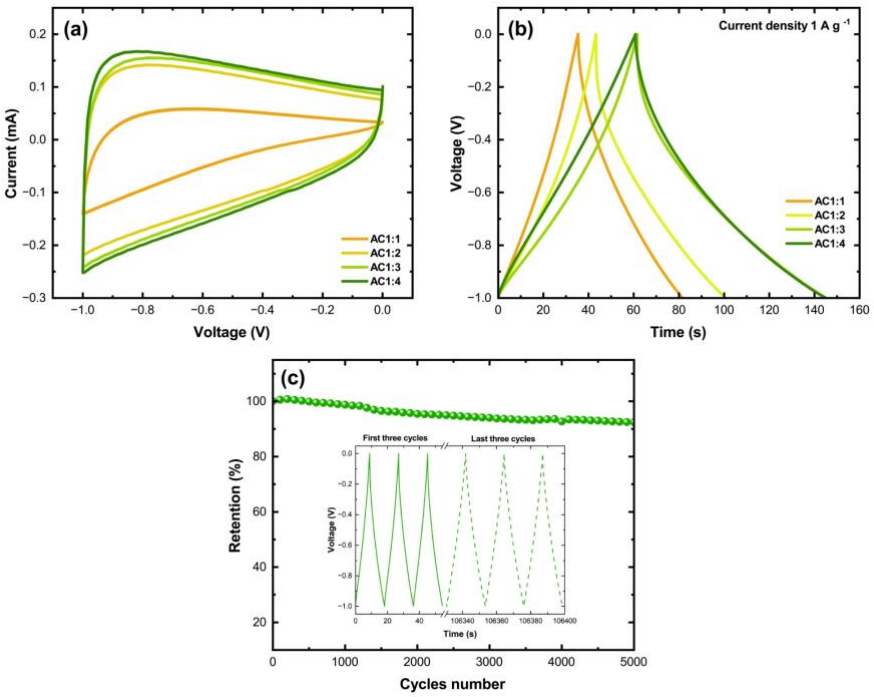

Fig. 5. (a) Comparative CV curves at a scan rate of 100 mV s^{-1} and (b) GCD curves at a current density of 1 A g^{-1}, and (c) capacitance retention of AC1:4 electrode at a current density of 10 A g^{-1} over 5,000 cycles.

4 Conclusion

ACs were successfully synthesized via a two-step process, including carbonization at 600 ºC followed by chemical activation at 800 ºC using varying ratios of $ZnCl_2$ (1:1, 1:2, 1:3, and 1:4). Characterization results showed that the ACs exhibited an amorphous structure without impurity phases, and the chemical functional groups were effectively removed after activation at high temperatures. The increase in $ZnCl_2$ content slightly influenced the creation of additional micropores and enhanced the surface area of ACs by 8%. Electrochemical measurements revealed that AC1:4 exhibited the highest specific capacitance of 56 F g^{-1} among all tested ACs. This was attributed to its highest specific surface area contributed by an increased presence of micropores. After a stability test for 5,000 charge-discharge cycles, the retention remained at 92%, demonstrating its excellent stability for prolonged operational use. Although the specific surface area and capacitance values were relatively low compared to reported ACs in the literature, this study highlights the potential of utilizing corncob waste as a precursor for AC production in supercapacitor electrodes. Future research will focus on optimizing other factors and refining the activation conditions to enhance the specific surface area and porosity of these ACs, making them more suitable for practical applications in supercapacitors.

5 Acknowledgments

This work was financially supported by the Kasetsart University Research and Development Institute (KURDI, grant no. FF(KU) 51.67) and the Innovation Development Scholarship for Master's students from the Faculty of Engineering, Kasetsart University (67/05/MAT/Innovation). The authors would also like to thank the Department of Materials Engineering and the Materials Innovative Center at Kasetsart University for their support in providing facilities and instruments.

References

[1] Mardani, A., Jusoh, A., Zavadskas, E.K., Cavallaro, F., Khalifah, Z.: Sustainable and renewable energy: An overview of the application of multiple criteria decision making techniques and approaches. Sustainability 7(10), 13947–13984 (2015).

[2] Mitali, J., Dhinakaran, S., Mohamad, A.A.: Energy storage systems: A review. Energy Storage and Saving 1, 166–216 (2022).

[3] Afif, A., Rahman, S.MH., Azad, A.T., Zaini, J., Islan, M.A., Azad, A.K.: Advanced materials and technologies for hybrid supercapacitors for energy storage–A review. Journal of Energy Storage 25, 100852 (2019).

[4] Sharma, S., Chand, R.: Supercapacitor and electrochemical techniques: A brief review. Results in Chemistry 5, 100885 (2023).

[5] Arumugam, B., Mayakrishnan, G., Manickavasagam, S.K.S., Kim, S.C., Vanaraj, R.: An overview of active electrode materials for the efficient high-performance supercapacitor application. Crystals 13(7), 1118 (2023).
[6] Park, H.W., Roh, K.C.: Recent advances in and perspectives on pseudocapacitive materials for supercapacitors-A review. Journal of Power Sources 557, 232558 (2023).
[7] Luo, L., Lan, Y., Zhang, Q., Deng, J., Luo, L., Zeng, Q., Gao, H., Zhao, W.: A review on biomass-derived activated carbon as electrode materials for energy storage supercapacitors. Journal of Energy Storage 55, 105839 (2022).
[8] Chen, M., Kang, X., Wumaier, T., Dou, J., Gao, B., Han, Y., Xu, G., Liu, Z., Zhang, L.: Preparation of activated carbon from cotton stalk and its application in supercapacitor. Journal of Solid State Electrochemistry 17(4), 1005–1012 (2013).
[9] Deng, J., Xiong, T., Wang, H., Zheng, A., Wang, Y.: Effects of cellulose, hemicellulose, and lignin on the structure and morphology of porous carbons. ACS Sustainable Chemistry & Engineering 4(7), 3750–3756 (2016).
[10] Lesbayev, B., Auyelkhankyzy, M., Ustayeva, G., Yeleuov, M., Rakhymzhan, N., Maltay, A., Maral, Y.: Recent advances: Biomass-derived porous carbon materials. South African Journal of Chemical Engineering 43, 327–336 (2023).
[11] Gong, J., Li, J., Xu, J., Xiang, Z., Mo, L.: Research on cellulose nanocrystals produced from cellulose sources with various polymorphs. RSC Advances 7, 33486 (2017).
[12] Abdallah, F., Arthur, E.K., Mensah-Darkwa, K., Gikunoo, E., Baffour, S.A., Agamah, B.A., Nartey, M.A., Agyemang, F.O.: Electrochemical performance of corncob-derived activated carbon-graphene oxide and TiO_2 ternary composite electrode for supercapacitor applications. Journal of Energy Storage 68, 107776 (2023).
[13] Wanprakhon, S., Pattaraphutanon, P., Borvornsudhasin, P., Choocherd, N.: Chemical and surface properties of activated carbon from banana peel by dry chemical activation. Journal of Materials Science and Applied Energy 10(3), 96–105 (2021).
[14] Ozdemir, I., Sahin, M., Orhan, R., Erdem, M.: Preparation and characterization of activated carbon from grape stalk by zinc chloride activation. Fuel Processing Technology 125, 200–206 (2014).
[15] Thu, M.M., Chaiammart, N., Jongprateep, O., Techapiesancharoenkij, R., Thant, A.A., Saito, N., Panomsuwan, G.: Introducing micropores into carbon nanoparticles synthesized via a solution plasma process by thermal treatment and their charge storage properties in supercapacitors. RCS Advances 24, 16136–16144 (2023).